Cellular sex throughout the organism underlies somatic sexual differentiation

Chloé Hérault, Thomas Pihl, Bruno Hudry

nature communications

Article

https://doi.org/10.1038/s41467-024-51228-6

Cellular sex throughout the organism underlies somatic sexual differentiation

Received: 9 November 2023

Accepted: 1 August 2024

Published online: 13 August 2024

Check for updates

Chloé Hérault[1], Thomas Pihl[1] & Bruno Hudry[1]

Sex chromosomes underlie the development of male or female sex organs across species. While systemic signals derived from sex organs prominently contribute to sex-linked differences, it is unclear whether the intrinsic presence of sex chromosomes in somatic tissues has a specific function. Here, we use genetic tools to show that cellular sex is crucial for sexual differentiation throughout the body in *Drosophila melanogaster*. We reveal that every somatic cell converts the intrinsic presence of sex chromosomes into the active production of a sex determinant, a female specific serine- and arginine-rich (SR) splicing factor. This discovery dismisses the mosaic model which posits that only a subset of cells has the potential to sexually differentiate. Using cell-specific sex reversals, we show that this prevalence of cellular sex drives sex differences in organ size and body weight and is essential for fecundity. These findings demonstrate that cellular sex drives differentiation programs at an organismal scale and highlight the importance of cellular sex pathways in sex trait evolution.

Living organisms utilise two major biological strategies to create sexual dimorphisms in somatic tissues[1,2]. The first involves the development of male and female-specific glands and organs that produce systemic signals. These sex-specific organs can shape and maintain somatic sex differences over time, regardless of the sex of the receiving cells[3]. The second strategy is based on sex chromosomes and relies on cell-intrinsic mechanisms. In this case, sex-chromosomal genes create distinctions in equivalent differentiated cells in both males and females. Cellular sex plays a critical role in this strategy.

Our understanding of the significance of cellular sex is primarily based on the study of invertebrate model systems[4,5] such as *Drosophila melanogaster*[6–8]. In this particular species, sexual differentiation does not depend on gonadal hormones. Females possess two X chromosomes, while males have one X and one Y chromosome. The specific complement of sex chromosomes in a given cell triggers a splicing cascade that produces an RNA-binding protein called TransformerF (TraF)[9–15]. This protein is exclusively produced in female cells and regulates the splicing of exonic enhancers by indirect binding through its partner, Transformer 2 (Tra2)[16–26]. Unlike TraF, Tra2 is present in both sexes and binds directly to RNA through its RNA-binding domain. TraF and Tra2 influence splice site selection through their arginine- and serine-rich (RS) domains, with TraF's RS domain serving as a bridge between spliceosome components[22,27–29].

TraF is responsible for the sex-specific splicing of only two identified targets: *doublesex* (*dsx*)[10,30,31] and *fruitless* (*fru*)[32–40] (Fig. 1a). These two key factors shape the sexual dimorphisms observed in flies. Male-specific isoforms of *fru* (*fruM*) are essential for producing transcription factors expressed in specific neurons that underlie sexual orientation and aggression[32–39]. Both male (*dsxM*) and female (*dsxF*) forms of *dsx* RNA also encode transcription factors, but only a few direct Dsx targets are known[7,41]. DsxM plays a crucial role in regulating sexual behaviours by controlling the development of male-specific neurons[42]. DsxF is expressed in just 80 neurons in the female brain, while DsxM is expressed in around 300 neurons in males[43]. Interestingly, some of these male-specific neurons also co-express FruM.[40,44]. DsxF activates the expression of *yolk protein* (*Yp*) genes in fat body cells, necessary for egg growth[45], and also promotes pheromone production by regulating a desaturase called *desatF*[46]. Sex-specific development of the gonads is the last and key aspect of sexual differentiation that is regulated by *dsx/fru*[7,47] and conserved in diverse animal species. Both *dsx* and *fru* are only expressed in a subset of cells and are required at specific critical periods during development to build dimorphic structures[44,48–50]. Once established, their continuous expression in adulthood is

[1]Université Côte d'Azur, CNRS, Inserm, Institut de Biologie Valrose, Nice, France. e-mail: Bruno.HUDRY@univ-cotedazur.fr

https://doi.org/10.1038/s41467-024-51228-6

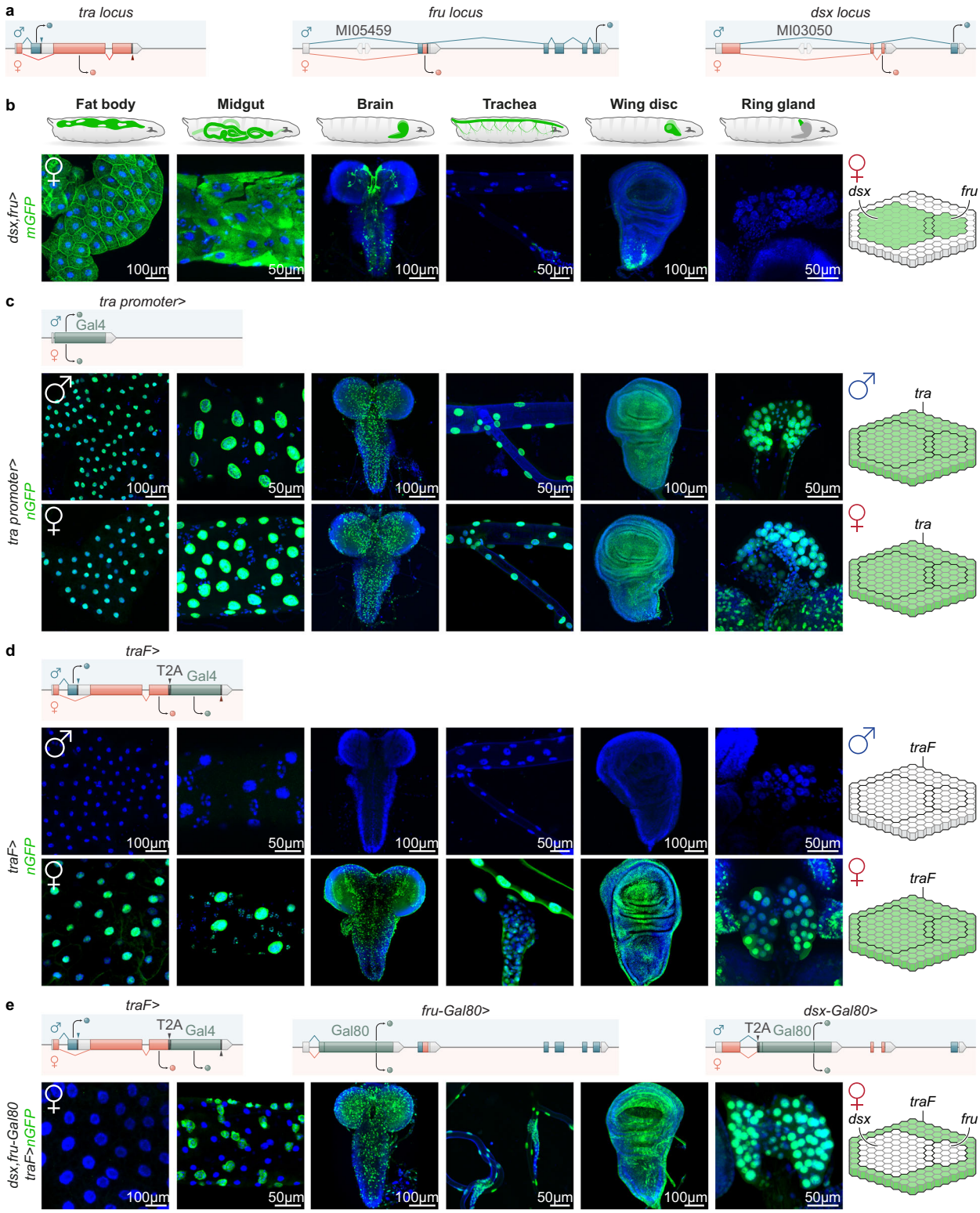

Fig. 1 | Every organ has a sexual identity. a Diagrams displaying the genomic loci of *tra*, *fru* and *dsx* genes. A blue and red triangle indicates the male- and female-specific stop coding in the *tra* locus. **b** Expression pattern of *dsx-Gal4* and *fru-Gal4* (*P1* promoter) reporters in female tissues at the third larval stage (DNA labelled with DAPI, blue; the membrane-bound form of GFP, green). **c** Expression pattern of *tra promoter-Gal4* reporter in male and female tissues at the third larval stage (DNA labelled with DAPI, blue; nucleus-targeted GFP, green). **d** Expression pattern of *traF-Gal4* reporter in male and female tissues at the third larval stage (DNA labelled with DAPI, blue; nucleus-targeted GFP, green). **e** Expression pattern of *traF-Gal4* reporter, combined with the *dsx-Gal80* and *fru-Gal80* (*P1* promoter) repressors, in female tissues at the third larval stage (DNA labelled with DAPI, blue; the nuclear form of GFP, green). The visualised cell populations and specific organs are green in the right and top diagrams. Diagrams of the new alleles generated are presented at the top of each panel. Immunohistochemical analyses were repeated at least three independent times.

sometimes needed to maintain sex differences. For example, thermosensitive alleles of *tra2* underscored the necessity of the sex cascade in sustaining sex-specific Yp synthesis[51,52] or *desatF* expression[41]. Adult gonadal cell types, intriguingly, also exhibit sexual plasticity. The continuous expression of DsxM in the adult testis' cyst cells is vital for preserving their sexual identity. Indeed, adult-specific ectopic DsxF production feminises these cells into female follicle-like cells[47,53]. Moreover, *dsx* and *fruM* function during adulthood to inhibit male-male courtship and maintain sexual orientation, respectively[54–56]. These results led to the proposal of the two-gene model of sexual differentiation[48]. According to this model, both male and female flies are composed of a mosaic of *dsx-/fru*-positive and *dsx-/fru*-negative cells that, consequently, have and don't have the potential to sexually differentiate. This mosaic expression of sexuality at the cellular level is believed to be a widespread feature of animals[57,58].

However, recent studies[59–61], including our work[62,63], have revealed that sex chromosomes impact the function of some cells, even if they do not express *dsx* and *fru*, the final effectors of the sex determination cascade. We previously found[62] that the sexual identity of adult intestinal stem cells, determined by the presence or absence of TraF, significantly impacts their proliferative capacity. These findings illustrate that somatic cells undergo sex-specific differentiation throughout adulthood, independently of *dsx* and *fru*. While we have established a proof-of-principle that TraF-dependent mechanisms impact intestinal stem cells, the full range of functions and phenotypic consequences of this sex pathway remains elusive.

Here, using newly generated *Drosophila melanogaster* genetic tools, we systematically assess the general significance of cellular sex at the organism-wide level. We found that every organ and somatic cell converts the intrinsic presence of sex chromosomes into the active production of a sex determinant. This ubiquity of cellular sex is crucial in determining sex differences in organ size and body weight. It is also essential for sex organ development and reproduction. Ultimately, our findings also show that these cellular sex pathways depend on the splicing activity of TraF and are active in *dsx*-expressing cells, where they control species-specific differentiation programmes vital for fertility. By testing the general role of cellular sex, we discover that it plays an essential function in the process of sexual differentiation.

Results

Every cell has a sexual identity

One outstanding question concerning the functioning of the sex determination cascade is whether all cells are sexually differentiated. Based on the expression of *dsx* and *fru*, the two terminal effectors of sexual differentiation (Fig. 1b)[44,48–50], most somatic tissues are the same in males and females and cannot differentiate sexually. Those observations suggest that TraF, the upstream sex determinant, lacks function in most organs. However, this hypothesis has never been tested: although *tra* was discovered in 1945[9], the lack of a functional TraF reporter has prevented further examination of *tra* expression and activity in most organs.

To test this assumption, we replaced *tra* coding sequences with Gal4 sequences, generating a transgenic reporter line and enabling us to follow *tra* promoter activity (Fig. 1c). As anticipated, we found that this knock-in Gal4 created a mutant allele of *tra* that produced classical tra^{KO} morphological phenotypes, female to male sex reversals, when heterozygous with a null allele (Supplementary Fig. S1a). Using this genetic tool, we first characterised the transcription pattern of *tra* at the third larval stage in all major tissues. Unlike *dsx* and *fru*, which are only expressed in a restricted subset of tissues (Fig. 1b), this reporter revealed ubiquitous *tra* expression across organs in both sexes (Fig. 1c).

To further investigate the specification of genetic sex at the organ level, we next examined the translation profile of the TraF protein. Previous work indicates that sex-specific splicing of *tra* transcripts only leads to the production of functional TraF protein in XX cells[7]. Therefore, we introduced *Gal4* in-frame just before the stop codon in the endogenous *tra* locus (Fig. 1d). The resulting allele, *traF-Gal4*, only produces wild-type TraF protein supporting female differentiation (Supplementary Fig. S1b) and Gal4 in females (Fig. 1d). We observed extensive TraF production in the tissues where *dsx* and *fru* are expressed, such as in the fat bodies (Fig. 1d), where DsxF activates *yolk protein* genes[45]. Interestingly, we also detected TraF in other female organs. For example, TraF is ubiquitously expressed in the female wing imaginal disc, the brain, and the tracheal system (Fig. 1d). We then characterised the temporal dynamics of *traF-Gal4*-driven expression. We found that TraF is ubiquitously produced at all developmental stages, from embryos to adults (Supplementary Fig. S1c).

To test whether somatic sexual identity based on TraF expression is independent of *dsx* and *fru*, we took advantage of Gal80-based repression of Gal4[64]. We generated a transgenic line where *dsx-Gal80* and *fru-Gal80* repress *traF-Gal4*-driven expression in *dsx*- and *fru*-positive cells. These two Gal80 alleles proved specific and efficient, suppressing *dsx*- and *fru-Gal4*-driven expression (Supplementary Fig. S1d, e). These tools were not able to suppress *traF-Gal4*-driven expression in most organs (Fig. 1e), validating the universality of cellular sex. While only a limited subset of tissues uses *dsx* and *fru* to differentiate sexually, our data indicate that cellular sex is ubiquitous, and most female organs have the potential to control their sexual differentiation through a mechanism downstream of TraF independent of classical *dsx*- and *fru*-based regulation.

We finally sought to characterise the dimorphic nature of *traF-Gal4*-driven expression at the cellular level. While our previous results demonstrated that every organ has its own sexual identity, it remains possible that some cells within a tissue (made of multiple cell types) do not have the capacity to sexually differentiate. To test this hypothesis, we introduced a different binary system to detect TraF production: *traF-LexA*. We combined this novel genetic tool with cell-type specific Gal4-UAS drivers and directly visualised the overlap between TraF expression and specific cell types. We selected two tissues for in-depth examination: the intestine and the brain. All the cell types studied (Fig. 2a and Supplementary Fig. S2a) expressed TraF in females only (Fig. 2b and Supplementary Fig. S2b). For example, all intestinal cell types (tracheal cells, visceral muscles, intestinal progenitors, and entero-endocrine cells) were negative for *dsx* and *fru* (Fig. 2c and Supplementary Fig. S2c) but positive for TraF during larval and adult stages (Fig. 2b and Supplementary Fig. S2b).

Taken together, our findings establish that cellular sex is ubiquitous both spatially and across developmental stages. Every somatic cell converts the intrinsic presence of sex chromosomes into the active production of the sex determinant TraF. This molecular switch specifies sexual state in a static and binary manner, with no organ, cell type, temporal plasticity or heterogeneity. This refutes the idea that males and females are mosaics of sexually differentiated and sexually undifferentiated cells.

Cellular sex is essential and sufficient to drive sex differences

Our results reveal that all cells are competent to differentiate sexually. Next we tested whether TraF expression reflects physiological differences in these cells. Is the effective action of the sex determination hierarchy limited only to a subset of cells? In *Drosophila*, based on the two-gene model of sexual differentiation[48], it is predicted that the conversion of both *dsx*- and *fru*-expressing cells should be enough to completely change an individual's phenotypic sex. We decided to test this model and assess the global functional significance of ubiquitous TraF expression.

To do so, we developed two new *tra* alleles, allowing us to perform conditional cis-allele switching[65] from a null allele of *tra* to the wild-type female isoform or the reverse. The first line, $tra^{KO\,FRT\,traF}$, allows the rescue of TraF activity following the expression of the Flp recombinase

https://doi.org/10.1038/s41467-024-51228-6

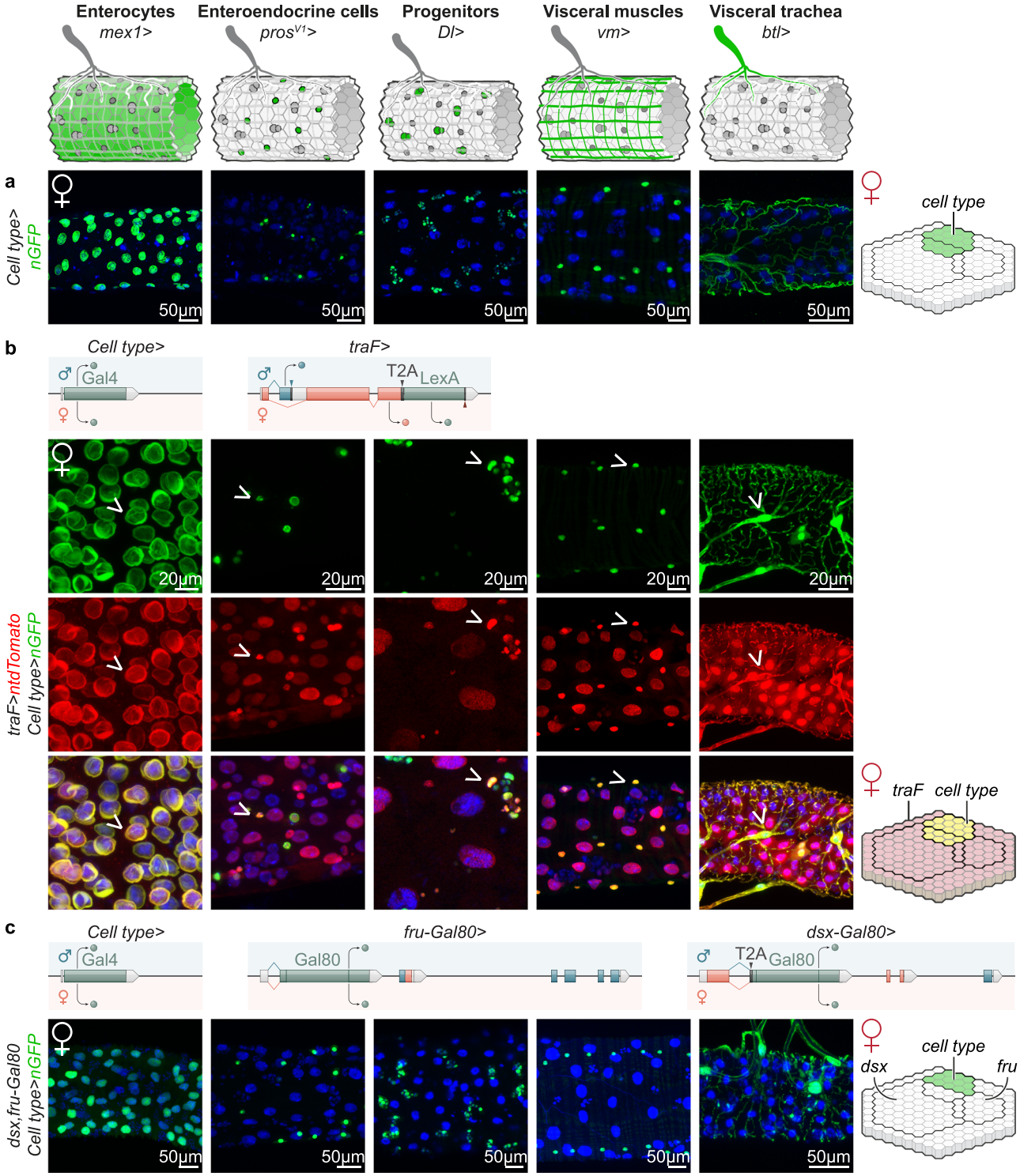

Fig. 2 | Every cell has a sexual identity. a Expression pattern of cell-type specific reporters in the female midgut at the third larval stage (DNA labelled with DAPI, blue; the nuclear form of GFP, green). **b** Expression pattern of cell-type specific reporters, combined with the *traF-LexA* marker, in the female midgut at the third larval stage (DNA labelled with DAPI, blue; the nuclear form of GFP, green, the nuclear form of tdTomato, red). Arrowheads indicate examples of cells expressing both GFP and tdTomato. **c** Expression pattern of cell-type specific reporters, combined with the *dsx-Gal80* and *fru-Gal80* repressors, in the female midgut at the third larval stage (DNA labelled with DAPI, blue; the nuclear form of GFP, green). The visualised cell populations and specific cell types are yellow or green in the right and top diagrams. The TraF-expressing cells alone and co-expressing cell-type specific markers are depicted in red and yellow, respectively. Diagrams of the alleles used are presented on the top of each panel. Immunohistochemical analyses were repeated at least three independent times.

in any cell type of interest. Combining this allele with *dsx-Gal4* and *fru-Gal4*-driven Flp expression generates *tra* knock-out females with restored *traF* expression, specifically in *dsx*- and *fru*-positive cells (Fig. 3a). The second line, $tra^{F\ FRT\ traKO}$, permits the production of TraF knock-in males. In this case, Flp expression in *dsx*- and *fru*-positive cells results in the expression of TraF in *dsx*- and *fru*-negative cells only (Fig. 3b). RT-qPCR and morphological analyses established that *dsx* and *fru* sex-specific splicing (Supplementary Fig. S3a, b), as well as

https://doi.org/10.1038/s41467-024-51228-6

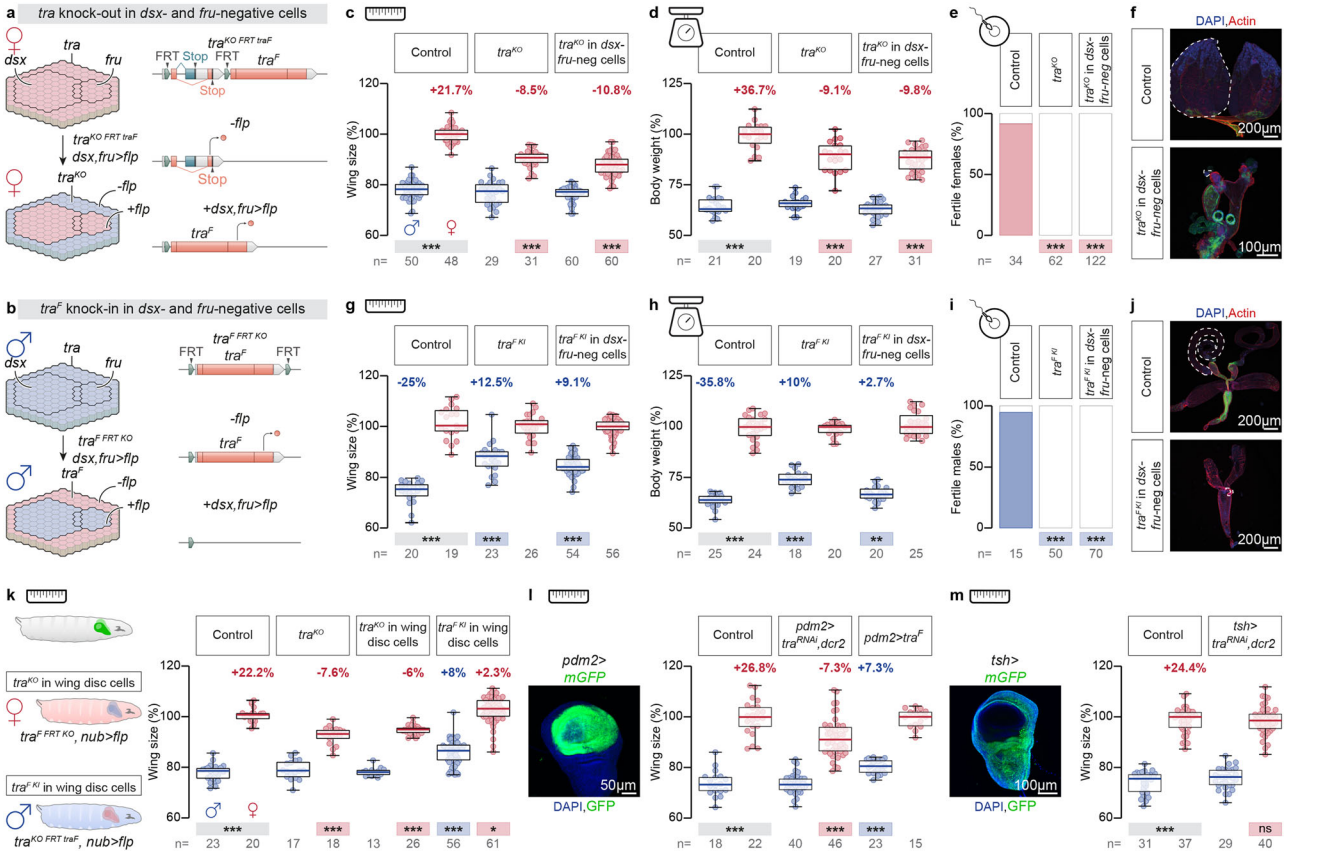

Fig. 3 | Cellular sex is essential and sufficient to drive sex differences. **a** Diagrams representing the specific cell population with *tra* knock-out in females, the allele generated and the genotypes used. **b** Diagrams representing the specific cell population with *traF* knock-in in males, the allele generated and the genotypes tested. **c**–**e** Adult wing size (**c**), adult weight (**d**), female fertility (**e**) quantifications following *tra* knock-out specifically in *dsx*- and *fru*-negative cells. In all figures, the wing size and the weight of control females are set at 100%. All other sexes and genotypes are shown as a percentage of this female control. **f** Ovaries of control females and females with *tra* knock-out specifically in dsx- and fru-negative cells (DNA labelled with DAPI, blue; Actin stained with phalloidin, red). **g**–**i** Adult wing size (**g**), adult weight (**h**), and male fertility (**i**) quantifications following *traF* knock-in specifically in *dsx*- and *fru*-negative cells. **j** Testes of control males and males with *traF* knock-in specifically in dsx- and fru-negative cells (DNA labelled with DAPI, blue; Actin stained with phalloidin, red). **k**–**m** Adult wing size quantifications following *tra* knock-out and gain-of-function specifically in wing pouch cells (**k**), *tra* knock-down and overexpression in wing pouch cells (**l**), and *tra* knock-down specifically in wing cells outside the pouch (**m**). In this and all subsequent figures, boxplots display the minimum, the maximum, the sample median, and the first and third quartiles. Data was combined from at least three independent experiments. *n* = wing number measured per genotype in (**c**), (**g**), (**k**), (**l**), and (**m**), number of replicates (each repeat containing five flies) in (**d**) and (**h**) and number of flies in (**e**) and (**i**). Asterisks highlighting significant comparisons across sexes are displayed in grey boxes at the bottom of graphs; those highlighting significant comparisons within female and male datasets are displayed in red and blue boxes, respectively. When significant, the difference compared to the median of the controls is indicated. For all panels, *p*-values from one-sided Mann-Whitney-Wilcoxon tests are ***$p < 0.0001$, **$p = 0.0043$, *$p = 0.035$, (ns) $p = 0.7322$.

sex-specific abdominal pigmentation and genitalia (Supplementary Fig. S3c, d), remained unaffected validating that our manipulations were indeed restricted to *dsx*- and *fru*-negative cells. Based on these findings, we concluded that the modifications introduced into the *tra* locus generated chimeric male/female animals with manipulation of sexual identity confined to *dsx*- and *fru*-negative cells.

First, we investigated whether female differentiation requires cellular sex outside the cells expressing the only two known splicing targets of TraF. If so, females masculinised only in *dsx*- and *fru*-negative cells should display altered sexual differentiation. To test this prediction, we used our *tra*$^{KO\ FRT\ traF}$ allele to specifically express TraF in *dsx*- and *fru*-expressing cells (Fig. 3a). We used three sexually distinct characteristics, organ size, body weight, and fertility, to assess the phenotypic sex of the flies[59,66,67]. Knock-out of *tra* in *dsx*- and *fru*-negative cells resulted in partial masculinisation of organ size (Fig. 3c) and body weight (Fig. 3d). Indeed, females were ~10% smaller and lighter. The same manipulation sterilised females (Fig. 3e) due to the presence of atrophic gonads (Fig. 3f). Importantly, the phenotypes observed for the three readouts fully recapitulated *tra* null mutant phenotypes (Fig. 3c–e). Together, these data establish that a non-canonical TraF-dependent mechanism is essential and controls important aspects of somatic sexual differentiation in *dsx*- and *fru*-negative cells.

If cellular sex is a switch mechanism, then males feminised only in *dsx*- and *fru*-negative cells should not only lose male identity, but they should also gain female characteristics (Fig. 3b). We used our *tra*$^{F\ FRT\ traKO}$ allele to drive *traF* expression specifically in *dsx*- and *fru*-negative cells in males. This specific TraF expression resulted in increased wing size (Fig. 3g) and body weight (Fig. 3h), and induced male sterilisation (Fig. 3i) due to atrophic testes (Fig. 3j). Overexpression of TraF in *dsx*- and *fru*-negative cells recapitulated these observations and similarly induced female characteristics in otherwise normal males (Supplementary Fig. S3e–j). Interestingly, performing the reverse experiments, feminising males only in *dsx*- and *fru*-expressing cells (Supplementary Fig. S3k) did not affect organ size and body weight (Fig. 3c, d). These results confirm that the sexual identity of *dsx*- and *fru*-positive cells are not involved at all in the sex differences studied.

To investigate the mechanism of action of this new non-canonical sex pathway (i.e., independent of *fru* and *dsx*), we examined the relative contribution of cell-autonomous versus non-cell-autonomous

https://doi.org/10.1038/s41467-024-51228-6

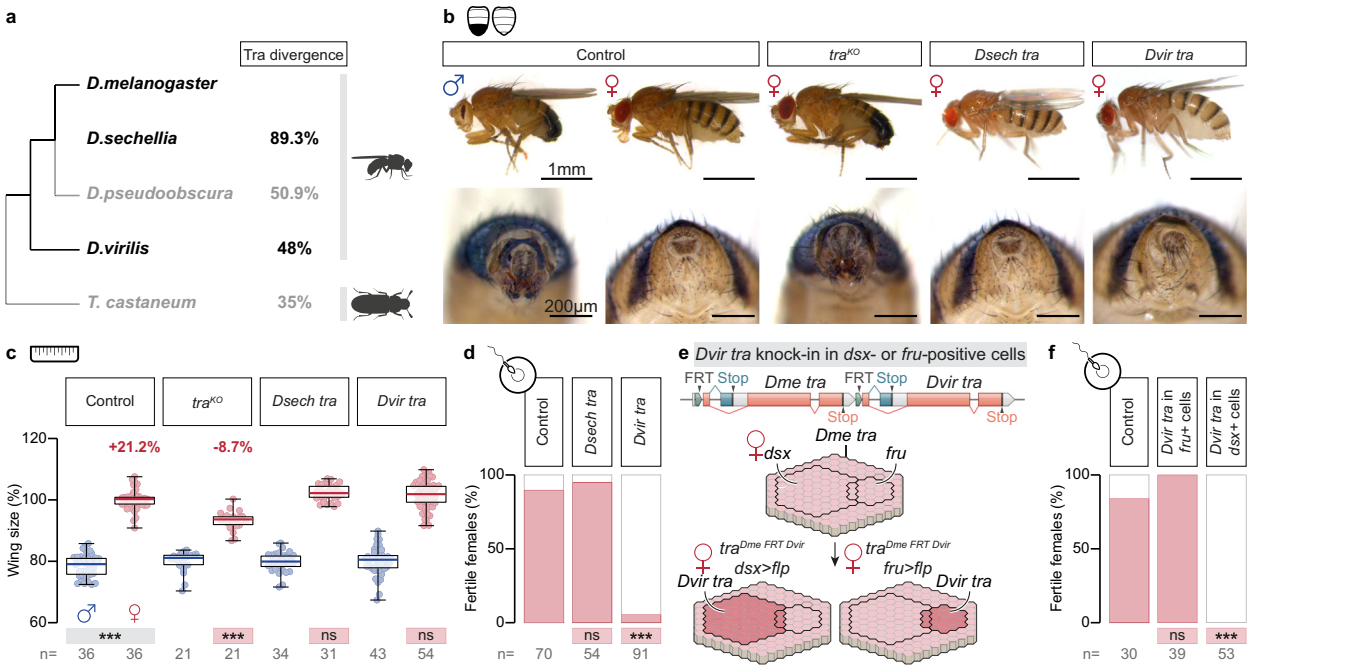

Fig. 4 | The TraF-dependent mechanism is active in *dsx*-expressing cells. a TraF protein sequence divergence between *Drosophila* species and the red flour beetle *Tribolium castaneum*. **b** Sex transformations of abdominal pigmentation and genitalia induced by *tra* knock-out and knock-in of *D. sechellia* and *D. virilis tra* genes. **c**, **d** Adult wing size (**c**), and female fertility (**d**) quantifications following *D. sechellia* and *D. virilis* TraF protein expressions. **e** Diagrams representing the specific cell population with *D. virilis tra* expression, the allele generated, and the genotypes tested. **f** Female fertility quantifications following *D. virilis* TraF protein expression specifically in *fru*- or *dsx*-positive cells. Data was combined from at least three independent experiments. *n* = wing number measured per genotype in (**c**) and number of flies in (**d**) and (**f**). Asterisks highlighting significant comparisons across sexes are displayed in grey boxes at the bottom of graphs; those highlighting significant comparisons within female datasets are displayed in red. For all panels, *p*-values from one-sided Mann-Whitney-Wilcoxon tests are ***$p < 0.0001$, (ns) $p > 0.066$.

effects of TraF on the sex differences in adult organ size. When we specifically eliminated or introduced *traF* function in the wing pouch cells, it significantly impacted wing size (Fig. 3k), mirroring whole-body *traF* manipulations (Fig. 3c, g). Interestingly, when we expressed *traF* only in the wing disc of a *traF* null mutant, it completely restored the standard size of female wings (Fig. 3k) despite all other organs being masculinised in these individuals. In fact, the adult wing was even slightly larger than that of wild-type females. We observed the same effects with both *traF* knockdown and over-expression, specifically in the wing disc (Fig. 3l). On the other hand, removing *traF* from all wing disc cells except the pouch didn't affect wing size (Fig. 3m). These results show that TraF's influence on the size of adult organs is primarily through cell-autonomous mechanisms. To strengthen our findings, we conducted genetic experiments targeting adipocytes, as a previous report suggested that the expression of TraF in the fat body could impact body size during larval stages in a non-cell-autonomous manner[59]. As anticipated from our earlier results, eliminating *traF* function in the fat body had no impact on wing size (Supplementary Fig. S3l). Furthermore, the expression of *traF* in adipocytes did not restore the size of female null mutants (Supplementary Fig. S3l). Similarly, both fat body-specific *traF* knockdown and over-expression did not affect wing size (Supplementary Fig. S3m), confirming that TraF controls the size of adult organs through cell-autonomous mechanisms.

Based on our observations, it appears that TraF exerts its splicing activity in a wide range of cells, including some that do not express *fru* or *dsx*. The expression of TraF in these cells is necessary and sufficient to shape multiple phenotypic differences between the sexes, through autonomous mechanisms. Indeed, we found that the sexual differentiation of the *dsx*- and *fru*-negative cells controls sex differences in organ size, body weight and sex organ formation. This is the first time that the sex of general somatic cells has been implicated in the three phenotypes investigated. It is a common biological strategy to use the sexual identity of equivalent differentiated cells in both sexes to create sex differences in phenotypes. Contrary to the traditional two-gene model of sexual differentiation that only considers *dsx*- and *fru*-positive cells, our findings indicate that cellular sex has a crucial role in organs and suggest that an intrinsic sex pathway exists downstream of TraF.

The new TraF-dependent mechanism is active in *dsx*-expressing cells

Our previous genetic manipulations were restricted to *dsx*- and *fru*-negative cells, so we were curious to test whether TraF-dependent sex differentiation is active and operates in *dsx*- or *fru*-expressing cells.

We hypothesised that a TraF variant could potentially uncouple canonical and uncharacterised sex differentiation pathways, enabling us to test the latter's significance in *dsx*- and *fru*-cells. Given the high degree of evolutionary divergence in sex-determining gene sequences between species[68–70], we leveraged natural TraF variations among closely related fly species[71] (Fig. 4a). We generated knock-in lines that replaced the coding sequences of *D. melanogaster* TraF with sequences from two closely related species, *D. sechellia* and *D. virilis*. These alleles were then evaluated to determine their ability to regulate various aspects of sexual differentiation under TraF control. *D. sechellia* protein was able to rescue all aspects of female differentiation, including genitalia formation (Fig. 4b), *dsx*, and *fru* splicing (Supplementary Fig. S4a), as well as organ size (Fig.4c) and female fertility (Fig. 4d). However, while the *D. virilis* protein triggered *dsx* and *fru* female-specific splicing (Fig. 4b and Supplementary Fig. S4a) and female size (Fig. 4c), it failed to support female fertility (Fig. 4d). To confirm these findings, we generated two additional *tra* knock-in lines. One line was a negative control and utilised a more distantly related species, the beetle *Tribolium castaneum*[72]. The other line used the TraF protein

from *D. pseudoobscura*, which has a similar degree of divergence from *D. melanogaster* TraF as the *D. virilis* protein. The knock-in line from *T. castaneum* exhibited classical *tra* loss-of-function morphological phenotypes (Supplementary Fig. S4b), failing to induce female-specific splicing of *dsx* and *fru* (Supplementary Fig. S4a), as well as female organ size (Supplementary Fig. S4c) or fertility (Supplementary Fig. S4d). This allele served as a negative control for our cross-species transgenic approach. Interestingly, the *D. pseudoobscura* protein triggered female-specific splicing of *dsx* and *fru* (Supplementary Fig. S4a), as well as female size (Supplementary Fig. S4c), but it could not support female fertility (Supplementary Fig. S4d). This new allele independently replicated our results obtained with *D. virilis*. As anticipated, our approach identified TraF variants that can regulate *dsx* and *fru* splicing but can only partially activate the new TraF-based non-canonical sex differentiation pathway (i.e., independent of *fru* and *dsx*). This allows us to test its significance in *dsx*- and *fru*-expressing cells.

To establish how TraF divergence is linked to specific functions, we created a genetic tool to achieve tissue-specific interspecies gene exchange analyses. This transgenic fly line allowed us to replace the wild-type *D. melanogaster tra* gene with the divergent *tra* of *virilis* in any given genetically defined (Gal4-positive) cell population (Fig. 4e). While expression of *virilis* TraF specifically in *fru*-positive cells did not affect fertility (Fig. 4f), it sterilised females in *dsx*-positive cells (Fig. 4f). To rule out a potential effect of altered *dsx* splicing undetectable in RT-qPCR, we generated a *dsxF* constitutive allele ($dsxF^{cons}$). As expected, this new reagent was able to carry out all the crucial functions mediated by DsxF during development and adulthood (Supplementary Fig. S4e-j), which are necessary for female differentiation. Indeed, $dsxF^{cons}$ effectively suppressed the expression of a male-specific reporter[73] in the ventral nerve cord (Supplementary Fig. S4h) and simultaneously triggered the female-specific expression of *Yp1* in adult adipocytes in both males and females (Supplementary Fig. S4g). It also successfully restored the fertility of *dsx* null mutant females (Supplementary Fig. S4j). However, this feminising allele did not rescue the sterility of females expressing *D. virilis* TraF protein (Supplementary Fig. S4j), indicating that a sex pathway downstream of TraF is active and crucial in *dsx*-cells. We observed that these female flies had normal ovaries with developing egg chambers at all stages, including late vitellogenic stages (Supplementary Fig. S4k). However, they were unable to lay eggs and had swollen abdomens (Fig. 4b). The Hox gene *Abdominal-B* (*Abd-B*) is responsible for forming the posterior segments, which include cells involved in egg-laying behaviour, such as the motoneurons that innervate the oviducts[74] or the vaginal plate[75,76]. When *D. virilis* TraF was expressed specifically in *Abd-B*-expressing cells, it caused sterility in females (Supplementary Fig. S4l), suggesting that the egg retention phenotype might be due to problems in the sexual differentiation of these somatic cells.

These findings demonstrate that the cellular sex pathway we identified plays a crucial role not only during development in *dsx*- and *fru*-negative cells but also in *dsx*-positive cells. The cross-species transgenic tests provide evidence that the variation in TraF protein sequences between *Drosophila* species has functional importance and regulates lineage-specific cellular sex differentiation programmes.

Cellular sex requires the splicing activity of TraF and its cofactor Tra2

Previous experiments revealed that *D. virilis* TraF can splice *dsx* and *fru*, but only partially supports the activation of the cellular sex pathway. This led us to wonder if the new targets of TraF were also regulated at the splicing level. To gain further insights into the molecular mechanisms involved in cellular sex specification, we investigated whether TraF splicing activity is required. We therefore focused on the RS domain of TraF and its cofactor Tra2.

To eliminate TraF's splicing activity, we designed a new *tra* knock-in allele with RS/SR repeats mutated to alanines. Our findings showed that the absence of female-specific *dsx*- and *fru*-splicing events (Supplementary Fig. S5a) caused sex-reversal of genitalia and secondary sexual characteristics (Fig. 5a). We also observed a reduction in organ size (Fig. 5b) and body weight (Fig. 5c) in these masculinised female flies lacking the TraF RS domain. In addition, these pseudo-males were found to be sterile (Fig. 5d). Notably, deletion of the C-terminal proline-rich domain, which is not implicated in the splicing activity of TraF[27], did not impact the ability of TraF to drive female organ size, unlike RS domain mutation (Supplementary Fig. S5b). These results highlight that the RS domain is required for TraF splicing activity and its role in cellular sex-driven differentiation.

We then tested whether Tra2 protein, the binding partner of TraF, is involved in the regulation of cellular sex. To study its expression pattern, we generated a *tra2-Gal4* knock-in reporter line (Fig. 5e). Our findings showed that when *tra2* knockdown was induced through *tra2-Gal4*, female-to-male sex reversal transformations occurred in all sexually dimorphic structures controlled by *dsx* and *fru* (Supplementary Fig. S5c). This effect could be rescued when *tra2-Gal4* was combined with *dsx*- and *fru-Gal80* (Supplementary Fig. S5c). All of our findings were consistent with *tra2-Gal4* accurately reporting *tra2* expression. We also found that this newly generated reporter was expressed ubiquitously in both sexes (Fig. 5e and Supplementary Fig. S5d), suggesting that the sex differentiation pathway could also rely on Tra2.

In order to evaluate the role of Tra2, we introduced *tra2* into cells expressing *dsx* and *fru* in *tra2* null mutants. This approach allowed us to generate flies that specifically lack Tra2 in cells that do not express the two established splicing targets of TraF. We accomplished this using a *tra2* CRISPR null mutant and two lines that reinstated *tra2* expression in *dsx*- and *fru*-expressing cells (Fig. 5f). These lines were created by exchanging MiMIC lines[77] with a trojan exon encoding *tra2*. This genetic manipulation fully rescued sex-specific splicing of *dsx* and *fru* (Supplementary Fig. S5e) as well as genitalia formation (Supplementary Fig. S5f). In addition, we drove *tra2* knockdown using the newly generated *traF-Gal4* combined with *dsx*- and *fru-Gal80* as an alternative strategy (Supplementary Fig. S5g–k). Both genetic manipulations partially abrogated the sex bias in organ size (Fig. 5g and Supplementary Fig. S5j) and body weight (Fig. 5h and Supplementary Fig. S5k). The *tra2* mutation downregulates size and weight in masculinised female flies. Indeed, females were 8% smaller and 11% lighter, whereas males were unaffected. Moreover, we were able to abolish the feminisation of organ size and body weight in TraF overexpressing males by downregulating *tra2* expression (Supplementary Fig. S5l). These results suggest that the presence of Tra2 in somatic cells is crucial for the control of organ size and body weight by cellular sex. However, we observed that *tra2* mutation (Fig. 5i) and downregulation (Supplementary Fig. S5m) did not affect female fertility when confined to *dsx*- and *fru*-negative cells. This indicates that a distinct *tra2*-independent mechanism is involved in fertility control by cellular sex.

Thus, our data point to the existence of two cellular sex pathways that contribute to sex differences and depend on the RS domain of TraF. One mechanism is *tra2*-dependent and controls sex-specific differences in organ size and body weight, while the other mechanism is *tra2*-independent and is essential for female fertility.

Discussion

Our findings invalidate the two-gene model of sexual differentiation in *Drosophila* and demonstrate that cellular sex is ubiquitous and essential for shaping differences between males and females during development and evolution.

We found that every somatic cell expresses the primary sex determinant, TraF, indicating that all male and female cells are sexually differentiated. It is worth noting that among the thousand *Gal4* reporter lines generated in *Drosophila* over decades, our *traF-Gal4* is the first and only sex-specific and ubiquitous line. Obtaining this tool

https://doi.org/10.1038/s41467-024-51228-6

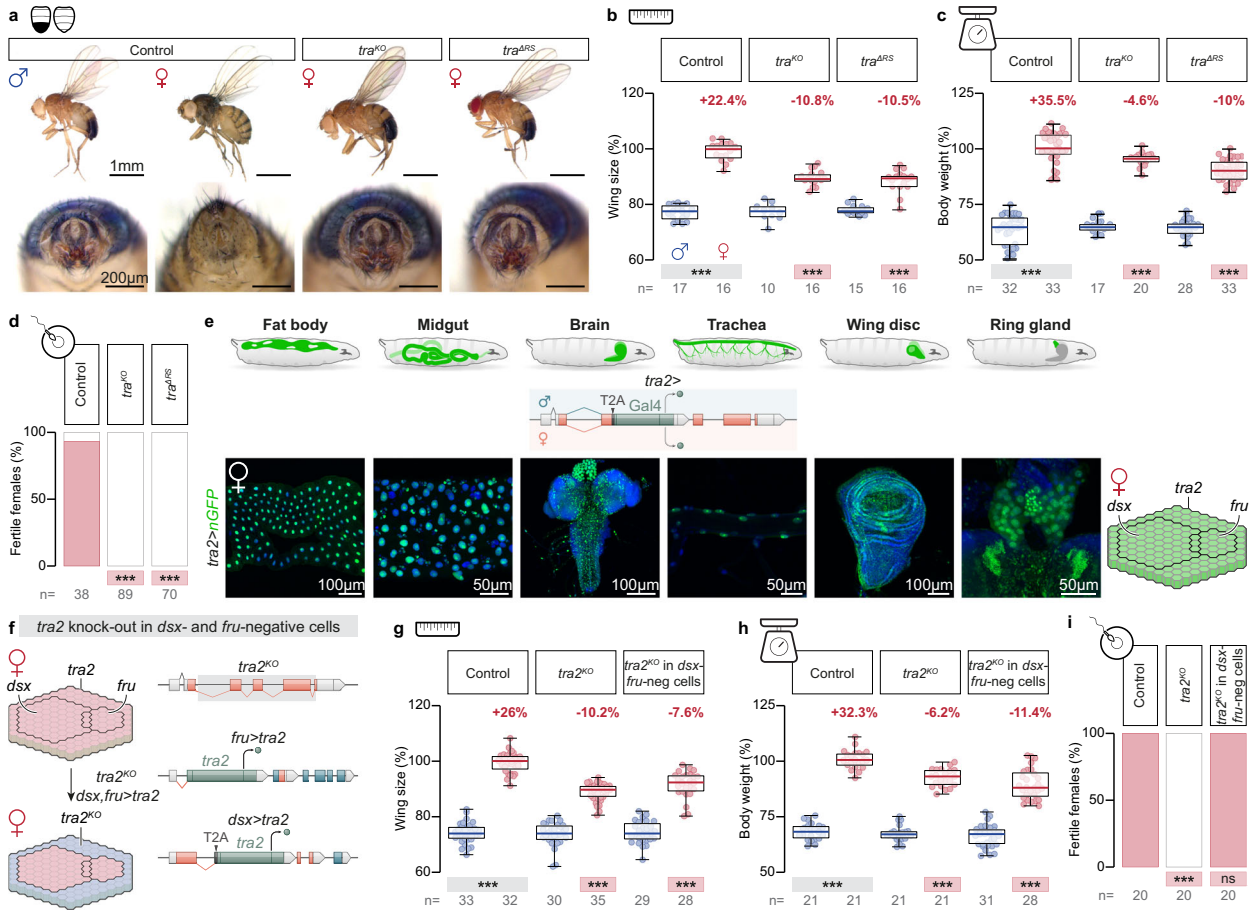

Fig. 5 | Cellular sex requires the splicing activity of TraF and its cofactor Tra2. **a** Sex transformations of abdominal pigmentation and genitalia induced by *tra* knock-out and RS domain mutation. **b**–**d** Adult wing size (**b**), adult weight (**c**), and female fertility (**d**) quantifications following RS domain mutation. **e** Expression pattern of *tra2-Gal4* reporter in the female tissues at the third larval stage (DNA labelled with DAPI, blue; the nuclear form of GFP, green). **f** Diagrams representing the specific cell population with *tra2* knock-out, the alleles generated, and the genotype used. **g**–**i** Adult wing size (**g**), adult weight (**h**), and female fertility (**i**) quantifications following *tra2* knock-out specifically in *dsx*- and *fru*-negative cells. Data was combined from at least three independent experiments. *n* = wing number measured per genotype in (**b**) and (**g**), number of replicates (each repeat containing five flies) in (**c**) and (**h**) and number of flies in (**d**) and (**i**). Asterisks highlighting significant comparisons across sexes are displayed in grey boxes at the bottom of graphs; those highlighting significant comparisons within female datasets are displayed in red. For all panels, *p*-values from one-sided Mann-Whitney-Wilcoxon tests are $^{***}p < 0.0001$, (ns) $p > 0.99$.

was quite challenging since TraF production is controlled by female-specific alternative splicing of a very short exon, an event easily disrupted by the introduction of additional sequences. The ubiquitous expression of the fly sex determinant has significant implications beyond sex differentiation. TraF is a splicing factor, thus it appears crucial to sex biological samples when studying alternative splicing processes in *Drosophila*. In the brain, for example, all neuronal and glial cells expressed TraF, and this tissue has the maximum mRNA isoform diversity, but most splicing studies[78,79] still use unisex or mixed samples. Besides fundamental research, our observation could be beneficial for genetic engineering. For example, individual sex-sorting remains a crucial issue in male sterile techniques developed to control pests and disease vector insect populations[80]. Our *traF-Gal4* line design could serve as a model for developing reporters that combine fluorescent proteins downstream of the ubiquitous female-specific *traF* exon. This approach could be adapted to various insect species since TraF is conserved.

While recent studies suggest that non-cell-autonomous mechanisms also contribute to male-female size differences in flies[59,81–83], our data reveal that intrinsic sex pathways downstream of TraF account for 40% of sex difference in organ size and 30% of the sex gap in body weight. Previous studies have primarily concentrated on analysing the targets and expression sites of *dsx* and *fru*[7], assuming that these two effectors account for all TraF functions. However, our discoveries emphasise that it is crucial to look beyond these two factors and characterise the complete range of sex-specific isoforms since the overlooked sex pathways depend on the splicing activity of TraF.

We discovered that TraF targets beyond *dsx* are also crucial for specifying sex organs. Our experiments, involving TraF from various fly species, further confirmed this conclusion. We found that one TraF protein from *D. virilis* could splice *dsx* and *fru* but could not support female reproduction. These findings prove that there are intrinsic cellular sex pathways that differ between closely related species, which operate in *dsx*-positive cells. Altogether, our experiments demonstrate the global requirement of cellular sex for sexual differentiation and the presence of essential sex pathways. The genetic tools we have developed will help researchers further explore the functional significance of cellular sex in various sex differences related to immunity[84], metabolism[85], or development[85] that have yet to be fully understood.

Our results make *Drosophila* the first animal where the presence of cellular sex and its functional importance have been tested extensively at the organism level. Could the ubiquitous nature of sex-determinant expression and function be conserved in other animals, including mammals? While the general importance of intrinsic sex

pathways remains to be determined, clear examples already highlight the critical role of cellular sex in these animals. In humans, the functional equivalent of TraF is SRY which instructs embryonic gonads to develop into testes[86]. Interestingly, SRY is also present in various adult tissues outside the sex organs, including the lungs, heart, and liver, where its putative functions and targets remain to be fully explored[87]. Beyond SRY, while it's commonly believed that Y-chromosome genes are only expressed in the testis, recent studies have shown elevated Y-chromosome gene expression in non-reproductive tissues[88–92]. For example, *EIF1AY*, which encodes an essential translation initiation factor, is more abundant in male heart tissue than its X-linked homologue EIF1AX in female heart tissue at the protein level[92]. Combined with the recent discoveries linking Y-linked genes to cancer growth and immunotherapy[93–95], it is becoming increasingly evident that cellular sex also plays an essential role in mammalian development and physiology. Despite these few examples, the global importance of cellular sex in vertebrates at the organism level and its integration with better-characterised hormonal effects remain to be elucidated.

Methods

Fly strains and media

Gal4 drivers. *dsx-Gal4* (gift from C. Rezaval, generated by ref. 44, FlyBase ID: FBti0168641), *fruP1-Gal4* (BDSC: 66696, FlyBase ID: FBti0168666), *mex1-Gal4* (BDSC: 91368, FlyBase ID: FBti0213076), *prosV1-Gal4* (BDSC: 84276, FlyBase ID: FBti0010694), *Dl-Gal4* (BDSC: 45136, FlyBase ID: FBti0134190), *vm-Gal4* (BDSC: 48547, FlyBase ID: FBti0133125), *btl-Gal4* (BDSC: 66790, FlyBase ID: FBti0185389), *repo-Gal4* (BDSC: 7415, FlyBase ID: FBti0018692), *nSyb-Gal4* (BDSC: 51635, FlyBase ID: FBti0150361), *tra promoter-Gal4* (this study, see below for details), *traF-Gal4* (this study, see below for details), *dsx-Gal80* (this study, see below for details), *fruP1-Gal80* (this study, see below for details), *traF-LexA* (this study, see below for details), *tra2-Gal4* (this study, see below for details), *nubbin-Gal4* (BDSC: 84330, FlyBase ID: FBti0016825), *cg-Gal4* (BDSC: 7011, FlyBase ID: FBti0027802), *Yolk1-Gal4* (BDSC: 58814, FlyBase ID: FBti0164887), *R17G11-Gal4* (BDSC: 49275, FlyBase ID: FBti0133549), *Abd-B-Gal4* (BDSC: 55848, FlyBase ID: FBti0074266), *pdm2-Gal4* (BDSC: 49828, FlyBase ID: FBtp0057439), *tsh-Gal4* (BDSC: 3040, FlyBase ID: FBti0002787).

UAS transgenes. *UAS-Stinger* (BDSC: 84277, FlyBase ID: FBti0074589), *UAS-flp* (BDSC: 4539, FlyBase ID: FBti0012284), *UAS-traF* (BDSC: 4590, FlyBase ID: FBti0010566), *UAS-traF* (this study, see below for details), *UAS-traF$^{\Delta RS}$* (this study, see below for details), *UAS-traF$^{\Delta P}$* (this study, see below for details), *LexAop2-IVS-tdTomato.nls* (BDSC:66680, FlyBase ID: FBti0185294), *UAS-IVS-mCD8::GFP* (BDSC: 32186, FlyBase ID: FBti0131963), *UAS-IVS-mCD8::GFP* (BDSC: 32185, FlyBase ID: FBti0131931), *UAS-dicer2* (VDRC: 60007).

RNAi transgenes. *UAS-tra2^{RNAi}* (BDSC: 28018, FlyBase ID: FBti0128004), *UAS-tra^{RNAi}* (BDSC: 28512, FlyBase ID: FBti0127269).

Mutants. *tra^{KO}* (BDSC: 67412, FlyBase ID: FBti0186559), *tra$^{F\ FRT\ KO}$* (generated by ref. 63, FlyBase ID: FBti0211844), *tra$^{KO\ FRT\ traF}$* (this study, see below for details), *tra$^{\Delta RS}$* (this study, see below for details), *tra2^{KO}* (this study, see below for details), *dsx>tra2* (this study, see below for details), *fruP1>tra2* (this study, see below for details), *Dsech tra* (this study, see below for details), *Dvir tra* (this study, see below for details), *tra$^{Dmel\ FRT\ Dvir}$* (this study, see below for details), *dsx^{Fcons}* (this study, see below for details), *dsx^{1}* (BDSC: 1679, FlyBase ID: FBal0003154), *dsx$^{\Delta}$* (gift from B. Prudhomme, FlyBase ID: FBal0325111), *tra2^{1}* (BDSC: 66712, FlyBase ID: FBal0017020), *Df(3L)st-j7* (BDSC: 5416, FlyBase ID: FBab0002416), *Dpseudo tra* (this study), *Tcas tra* (this study).

Animals were reared on fly food containing (per liter): 10 g of agar, 82.5 g polenta, 34 g dry yeast and 3,75 g Moldex (per liter, diluted in ethanol). All experimental flies were kept in incubators at 25 °C, and on a 12 hr light/dark cycle. Flies were transferred to fresh vials every 3 days, and fly density was kept to a maximum of 15 flies per vial.

Fertility tests

For fertility experiments, males or females were collected and aged for 3–5 days. For female fertility experiments, females were mated over five days to CantonS males (1 female with 1 male per vial). For male fertility experiments, males were mated over five days to CantonS females (1 male with 3 females per vial). Flies were then removed, and progeny was counted.

Generation of the *tra promoter-Gal4* knock-in allele

To generate the *tra promoter Gal4* knock-in allele, the 1917 nucleotides (nt) upstream of the *tra* start codon were cloned into the RIV FRTnMCS1FRT white vector (DGRC: Plasmid#1333) using the NotI and NheI restriction sites by gene synthesis (Genscript). The Gal4 sequences and the 3'UTR of *tra*, along with the 967 downstream nt, were added by PCR between the NheI and XhoI sites. The construct was sequence-verified, and a transgenic line was established through ΦC-31 integrase mediated transformation (Bestgene), using a recently generated amorphic allele of *tra*[63] in which *tra* locus has been replaced by an attP site (BDSC: 67412, FlyBase ID: FBti0186559). The generated allele behaves as a *tra* null mutant.

Generation of the *traF-Gal4* and *traF-LexAp65* knock-in alleles

To generate the *traF-Gal4* and *traF-LexAp65* knock-in alleles, the *T2A-Gal4* sequences (Addgene: Plasmid #62893) or the *T2A-nls-LexA::p65* sequences (Addgene: Plasmid #26230) were cloned upstream of the *tra* STOP codon into an RIV FRTnMCS1FRT white vector (DGRC: Plasmid#1333, containing the *tra* locus (3869 nt containing: *tra* coding region, 1910 nt upstream and the 967 nt downstream[63]). The constructs were sequence-verified and transgenic lines were established through ΦC-31 integrase mediated transformation (Bestgene), using a recently generated amorphic allele of *tra*[63] in which *tra* locus has been replaced by an attP site (BDSC: 67412, FlyBase ID: FBti0186559).

Generation of the *traF^{KO}-Gal4* knock-in allele

To generate the *traF^{KO}-Gal4* knock-in allele, the *T2A-Gal4* sequences (Addgene: Plasmid #62893) were cloned 26 nt downstream of the *tra* female-specific exon into a RIV FRTnMCS1FRT white vector (DGRC: Plasmid#1333, containing the *tra* locus (674 nt containing: *tra* coding region deleted of 582 nt of the female-specific exons, the 353 nt upstream and the 310 nt downstream[63]). The constructs were sequence-verified and transgenic lines were established through ΦC-31 integrase mediated transformation (Bestgene), using a recently generated amorphic allele of *tra*[63] in which *tra* locus has been replaced by an attP site (BDSC: 67412, FlyBase ID: FBti0186559).

Generation of the *dsx-Gal80* knock-in allele

To generate a knock-in *Gal80* under the control of *dsx* regulatory sequences, recombination-mediated cassette exchange of the following insertion was performed: *Mi{y[+mDint2]=MIC}dsx[MI03050]* (BDSC: 36182, FlyBase ID: FBti0143242). The swapping strategy was previously described in ref. 77. Midiprep plasmid DNA of *pBS-KS-attB2-SA(1)-T2A-3X Gal80-Hsp70* (addgene: Plasmid#62952) was injected together with ΦC31 plasmid DNA into the embryos of flies bearing *MI03050*. The orientation of the Gal80 exon inserts was then determined by PCR amplification.

Generation of the *fru-Gal80* knock-in allele

To generate a knock-in *Gal80* under the control of *fru* regulatory sequences (P1 promoter), recombination-mediated cassette exchange of the following insertion was performed: *Mi{y[+mDint2]=MIC} fru[MI05459]* (BDSC: 42086, FlyBase ID: FBti0149046). Midiprep plasmid DNA of *pBS-KS-attB2-SA(1)-T2A-3X Gal80-Hsp70* (addgene:

Plasmid#62952) was injected together with ΦC31 plasmid DNA into the embryos of flies bearing *MI05459*. The orientation of the Gal80 exon inserts was then determined by PCR amplification.

Generation of the *UAS-traF* lines

To generate a wild type *UAS-traF* line, *tra* coding regions (687 nt, FlyBase ID: FBtr0075364) were cloned by PCR into the pUASt-attB vector (DGRC: Plasmid#1419) between the EcoRI and XhoI restrictions sites. In the *UAS-traF*$^{\Delta RS}$ line, the 17 RS/SR repeats are mutated in alanine (RS/SR > AA). In the *UAS-traF*$^{\Delta P}$ line, the 35 last amino-acids of *tra* are deleted. The constructs were sequence-verified and transgenic lines were established through ΦC-31 integrase mediated transformation (Bestgene), using the attP40 (BDSC: 36304, FlyBase ID: FBti0114379) attP site line.

Generation of the *tra*$^{KO\ FRT\ traF}$ knock-in allele

To generate the *tra*$^{KO\ FRT\ traF}$ knock-in allele, the following sequences were cloned into the RIV FRTnMCS1FRT white vector (DGRC: Plasmid#1333) using the EcoRI and BglII restriction sites by gene synthesis (Genscript): *tra promoter*-truncated *tra* cDNA –FRT site – *traF* cDNA. The construct was sequence-verified, and transgenic lines were established through ΦC-31 integrase mediated transformation (Bestgene), using a recently generated amorphic allele of *tra*[63] in which *tra* locus has been replaced by an attP site (BDSC: 67412, FlyBase ID: FBti0186559).

Generation of the *D. virilis tra* knock-in allele

To generate the *D. virilis tra* knock-in allele, the *tra* locus (*tra* coding region, the 353 nt upstream and the 310 nt downstream) was cloned by gene synthesis (Genscript) into the RIV FRTnMCS1FRT white vector (DGRC: Plasmid#1333) using the EcoRI and XhoI restriction sites. The *tra*-coding regions were replaced with the *tra*-coding regions of *D. virilis*. The introns, 5'UTR, and 3'UTR were not swapped. The construct was sequence-verified, and a transgenic line was established through ΦC-31 integrase-mediated transformation (Bestgene) using a recently generated amorphic allele of *tra*[63] in which the *tra* locus has been replaced by an attP site (BDSC: 67412).

Generation of the *D. sechellia tra* knock-in allele

To generate the *D. sechellia tra* knock-in allele, the *tra* locus (*tra* coding region, the 353 nt upstream and the 310 nt downstream) was cloned by gene synthesis (Genscript) into the RIV FRTnMCS1FRT white vector (DGRC: Plasmid#1333) using the EcoRI and XhoI restriction sites. The *tra*-coding regions were replaced with the *tra*-coding regions of *D. sechellia*. The introns, 5'UTR, and 3'UTR were not swapped. The construct was sequence-verified, and a transgenic line was established through ΦC-31 integrase mediated transformation (Bestgene) using a recently generated amorphic allele of *tra*[63] in which *tra* locus has been replaced by an attP site (BDSC: 67412).

Generation of the *D. pseudoobscura tra* knock-in allele

To generate the *D. pseudoobscura tra* knock-in allele, the *tra* locus (*tra* coding region, the 353 nt upstream and the 310 nt downstream) was cloned by gene synthesis (Genscript) into the RIV FRTnMCS1FRT white vector (DGRC: Plasmid#1333) using the EcoRI and NheI restriction sites. The *tra*-coding regions were replaced with the *tra*-coding regions of *D. pseudoobscura*. The introns, 5'UTR, and 3'UTR were not swapped. The construct was sequence-verified, and a transgenic line was established through ΦC-31 integrase mediated transformation (Bestgene) using a recently generated amorphic allele of *tra*[63] in which *tra* locus has been replaced by an attP site (BDSC: 67412).

Generation of the *T. castaneum tra* knock-in allele

To generate the *T. castaneum tra* knock-in allele, the *tra* locus (*tra* coding region, the 353 nt upstream and the 310 nt downstream) was cloned by gene synthesis (Genscript) into the RIV FRTnMCS1FRT white vector (DGRC: Plasmid#1333) using the EcoRI and XhoI restriction sites. The *tra*-coding regions were replaced with the *tra*-coding regions of *T. castaneum*. The introns, 5'UTR, and 3'UTR were not swapped. The construct was sequence-verified, and a transgenic line was established through ΦC-31 integrase mediated transformation (Bestgene) using a recently generated amorphic allele of *tra*[63] in which *tra* locus has been replaced by an attP site (BDSC: 67412).

Generation of the *tra*$^{Dmel\ FRT\ Dvir}$ knock-in allele

To generate the *tra*$^{Dmel\ FRT\ Dvir}$ knock-in allele, the following sequences were cloned into the RIV FRTnMCS1FRT white vector (DGRC: Plasmid#1333) using the EcoRI and XhoI restriction sites by gene synthesis (Genscript): *D. melanogaster tra locus*–FRT site – *D. virilis tra* locus. The construct was sequence-verified, and transgenic lines were established through ΦC-31 integrase-mediated transformation (Bestgene) using a recently generated amorphic allele of *tra*[63] in which *tra* locus has been replaced by an attP site (BDSC: 67412, FlyBase ID: FBti0186559).

Generation of the *dsxF*^{cons} knock-in allele

To generate a *dsx*^{Fcons} knock-in, recombination-mediated cassette exchange of the following insertion was performed: *Mi{y[+mDint2]=MIC}dsx[MI03050]* (BDSC: 36182, FlyBase ID: FBti0143242). The *pBS-KS-attB2-SA(1)-T2A-3X Gal80-Hsp70* (addgene: Plasmid#62952) vector was modified. The last common exon of *dsx* followed by the female-specific exon and the SV40 poly(A) replaced the *Gal80* sequences, and a 3xP3 promoter driving *DsRed* was added to facilitate the knock-in event screening. Midiprep plasmid DNA of this construct was injected together with ΦC31 plasmid DNA into the embryos of flies bearing *MI03050*. The orientation of the tra2 exon inserts was then determined by PCR amplification.

Generation of the *tra*$^{\Delta RS}$ knock-in allele

To generate the *tra*$^{\Delta RS}$ knock-in allele, the *tra* locus (1648 nt containing: *tra* coding region, the 353 nt upstream and the 310 nt downstream) was cloned by gene synthesis (Genscript) into the RIV FRTnMCS1FRT white vector (DGRC: Plasmid#1333) using the EcoRI and XhoI restriction sites. In the *tra* coding region, the 17 RS/SR repeats are mutated in alanine (RS > AA). The construct was sequence-verified, and a transgenic line was established through ΦC-31 integrase mediated transformation (Bestgene) using a recently generated amorphic allele of *tra*[63] in which *tra* locus has been replaced by an attP site (BDSC: 67412).

Generation of the *tra2*^{KO} CRISPR null mutant

To generate a *tra2* null mutant, two gRNAs targeting the *tra2* coding sequence (gRNA 1: tcgatgcttcatgtcaaaagagg, and gRNA 2: gatgaagttc-gacctaatcgtgg) were cloned into the pCFD5 vector (Addgene: Plasmid #73914). A 1 kb homology arm flanking the cleavage site 1 was PCR-amplified from genomic DNA using the Q5 high-fidelity polymerase from New England Biolabs (M0491S). The PCR product was digested with NheI and SacII prior to cloning into the pDsRedattP vector (Addgene: Plasmid #51019). A 1 kb homology arm flanking the cleavage site 2 was PCR-amplified from genomic DNA. The PCR product was digested with AvrII and XhoI prior to cloning into the pDsRedattP vector, containing the first homology arm. The constructs were sequence-verified and a mutant line was established through injection (Bestgene) of the 2 generated vectors (pCFD5 gRNAs and pDsRedattP homology arms) in *yw;nos-Cas9* (FlyBase ID: FBti0156858) embryos. The generated deletion removed 1513 nt of the *tra2* coding sequence and replaced it with an attP landing site and a loxP-flanked 3xP3-DsRed marker.

Generation of the *tra2-Gal4* knock-in allele

To generate the *tra2-Gal4* knock-in allele, the 589 nt of the *tra2* locus (containing half of the second intron and the third exon) were cloned into the RIV FRTnMCS1FRT white vector (DGRC: Plasmid#1333) using

the EcoRI and AsiSI restriction sites by gene synthesis (Genscript). The T2A-Gal4 sequences (addgene: Plasmid #62893), along the SV40 poly(A), were added by PCR between the AsiSI and XhoI sites. The construct was sequence-verified, and a transgenic line was established through ΦC-31 integrase mediated transformation (Bestgene), using a newly generated amorphic allele of $tra2^{KO}$ in which *tra2* locus has been replaced by an attP site. The generated allele behaves as *tra2* null mutant.

Generation of the *fru-tra2* knock-in allele

To generate a knock-in of *tra2* under the control of *fru* regulatory sequences (P1 promoter), recombination-mediated cassette exchange of the following insertion was performed: *Mi{y[+mDint2]=MIC} fru[MI05459]* (BDSC: 42086, FlyBase ID: FBti0149046). The *pBS-KS-attB2-SA(1)-T2A-3X Gal80-Hsp70* (addgene: Plasmid#62952) vector was modified. The *tra2* cDNA replaced the *Gal80* sequences, and a 3xP3 promoter driving *DsRed* was added to facilitate the knock-in event screening. Midiprep plasmid DNA of this construct was injected together with ΦC31 plasmid DNA into the embryos of flies bearing MI05459. The orientation of the tra2 exon inserts was then determined by PCR amplification.

Generation of the *dsx-tra2* knock-in allele

To generate a knock-in of *tra2* under the control of *dsx* regulatory sequences, recombination-mediated cassette exchange of the following insertion was performed: *Mi{y[+mDint2]=MIC}dsx[MI03050]* (BDSC: 36182, FlyBase ID: FBti0143242). The *pBS-KS-attB2-SA(1)-T2A-3X Gal80-Hsp70* (addgene: Plasmid#62952) vector was modified. The *tra2* cDNA replaced the *Gal80* sequences, and a 3xP3 promoter driving *DsRed* was added to facilitate the knock-in event screening. Midiprep plasmid DNA of this construct was injected together with ΦC31 plasmid DNA into the embryos of flies bearing *MI03050*. The orientation of the tra2 exon inserts was then determined by PCR amplification.

Immunohistochemistry

Larval and adult tissues were dissected in 1xPBS, placed on poly-L-lysine (Sigma-Aldrich, P1524-1G) coated slides, fixed in 3.7% formaldehyde (Polyscience) in 1xPBS for 20 min at room temperature (RT) and then washed several times in PBS containing 0,3% Triton X-100 (PBT). Dissected tissues were blocked in PBT + 4% Horse serum (HS) at RT for at least one h. The primary antibodies incubation was performed in PBT + HS for 48 h at 4 °C. After several washes, secondary antibodies were incubated for two hours at RT. Then, dissected tissues were mounted into Vectashield with DAPI (Vector Labs) to stain DNA. Fluorescence images were acquired using a Leica SP5 DS confocal microscope. The following primary antibodies (see also Table S1) were used: chicken anti-GFP (1/10000) (ab13970 Abcam), goat anti-tdTomato (1/500) (LS-C340696, LSBio).

Wing size

Adult flies were collected in ethanol at least 12 hours following emergence to ensure the wings were fully expanded. Right wings were dissected in ethanol and mounted in a drop of Euparal mounting medium (Carl Roth #7356.1). Slides were dried overnight on a heating plate at 60 °C. Then, wings were imaged using a Leica M205 FA associated with Leica DFC7000T camera. Wing areas were quantified using ImageJ by manually selecting the Cartesian coordinates of six landmarks representing junctions of veins with the wing contour, then measuring the number of pixels included in the resulting outline (method adapted from[96]). For a given experiment, all values were normalised to one control condition.

Body weight

2–5 days old male and female flies were frozen at −20 °C. During the two following days, flies were weighed by groups of 5 adults on an XPR analytical balance (Mettler Toledo). For a given experiment, all values were normalised to one control condition.

Reverse transcription and quantitative-PCR

RNAs were extracted from 10 whole flies (or 15 heads) using TRIzol (Invitrogen). RNAs were cleaned using an RNAeasy mini Kit (Qiagen, 74-104). cDNAs were synthesised using the iScript cDNA synthesis kit (Bio-Rad, 170-8889) from 500 ng of total RNAs. Quantitative PCRs were performed by mixing cDNA samples (5 ng) with iTaq Universal SYBR® Green Supermix (Bio-Rad, 172-5124) and the relevant primers in 384-well plates. Expression abundance was calculated using a standard curve for each gene and normalised to the expression of the rp49 control gene. For data display purposes, the median of the expression abundance was arbitrarily set at 100% for control males or females, and the percentage of that expression is displayed for all the tested genotypes. qPCR primer pairs used are listed in table S1.

Statistics and data presentation

All statistical analyses were carried out in GraphPad Prism 7.04. Comparisons between two genotypes or conditions were analysed with the Mann-Whitney-Wilcoxon rank sum test. This non-parametric test does not require the assumption of normal distributions, so no methods were used to determine whether the data met such assumptions. All graphs were generated using GraphPad Prism 7.04. In all figures, when significant, the differences between the medians of the control and the tested conditions are indicated.

Reporting summary

Further information on research design is available in the Nature Portfolio Reporting Summary linked to this article.

Data availability

All data is available in the main text or the supplementary materials. Materials generated for the study are available from the corresponding author on request. Source data are provided with this paper.

References

1. Arnold, A. P. Rethinking sex determination of non-gonadal tissues. *Curr. Top. Dev. Biol.* **134**, 289–315 (2019).
2. Arnold, A. P. Sexual differentiation of brain and other tissues: five questions for the next 50 years. *Horm. Behav.* **120**, 104691 (2020).
3. Mauvais-Jarvis, F., Arnold, A. P. & Reue, K. A guide for the design of pre-clinical studies on sex differences in metabolism. *Cell Metab.* **25**, 1216–1230 (2017).
4. García, L. R. & Portman, D. S. Neural circuits for sexually dimorphic and sexually divergent behaviors in Caenorhabditis elegans. *Curr. Opin. Neurobiol.* **38**, 46–52 (2016).
5. Meyer, B. J. Mechanisms of sex determination and X-chromosome dosage compensation. *Genetics* **220**, iyab197 (2022).
6. Hopkins, B. R. & Kopp, A. Evolution of sexual development and sexual dimorphism in insects. *Curr. Opin. Genet Dev.* **69**, 129–139 (2021).
7. Camara, N., Whitworth, C. & Van Doren, M. The creation of sexual dimorphism in the Drosophila soma. *Curr. Top. Dev. Biol.* **83**, 65–107 (2008).
8. Christiansen, A. E., Keisman, E. L., Ahmad, S. M. & Baker, B. S. Sex comes in from the cold: the integration of sex and pattern. *Trends Genet* **18**, 510–516 (2002).
9. Sturtevant, A. H. A gene in drosophila melanogaster that transforms females into males. *Genetics* **30**, 297–299 (1945).
10. Baker, B. S. & Ridge, K. A. Sex and the single cell. I. On the action of major loci affecting sex determination in Drosophila melanogaster. *Genetics* **94**, 383–423 (1980).
11. Belote, J. M. et al. Control of sexual differentiation in Drosophila melanogaster. *Cold Spring Harb. Symp. Quant. Biol.* **50**, 605–614 (1985).

12. Butler, B., Pirrotta, V., Irminger-Finger, I. & Nöthiger, R. The sex-determining gene tra of Drosophila: molecular cloning and transformation studies. *EMBO J.* **5**, 3607–3613 (1986).
13. McKeown, M., Belote, J. M. & Baker, B. S. A molecular analysis of transformer, a gene in Drosophila melanogaster that controls female sexual differentiation. *Cell* **48**, 489–499 (1987).
14. Boggs, R. T., Gregor, P., Idriss, S., Belote, J. M. & McKeown, M. Regulation of sexual differentiation in D. melanogaster via alternative splicing of RNA from the transformer gene. *Cell* **50**, 739–747 (1987).
15. McKeown, M., Belote, J. M. & Boggs, R. T. Ectopic expression of the female transformer gene product leads to female differentiation of chromosomally male Drosophila. *Cell* **53**, 887–895 (1988).
16. Ryner, L. C. & Baker, B. S. Regulation of doublesex pre-mRNA processing occurs by 3′-splice site activation. *Genes Dev.* **5**, 2071–2085 (1991).
17. Hoshijima, K., Inoue, K., Higuchi, I., Sakamoto, H. & Shimura, Y. Control of doublesex alternative splicing by transformer and transformer-2 in Drosophila. *Science* **252**, 833–836 (1991).
18. Inoue, K., Hoshijima, K., Higuchi, I., Sakamoto, H. & Shimura, Y. Binding of the Drosophila transformer and transformer-2 proteins to the regulatory elements of doublesex primary transcript for sex-specific RNA processing. *Proc. Natl Acad. Sci. USA* **89**, 8092–8096 (1992).
19. Tian, M. & Maniatis, T. Positive control of pre-mRNA splicing in vitro. *Science* **256**, 237–240 (1992).
20. Tian, M. & Maniatis, T. A splicing enhancer complex controls alternative splicing of doublesex pre-mRNA. *Cell* **74**, 105–114 (1993).
21. Amrein, H., Hedley, M. L. & Maniatis, T. The role of specific protein-RNA and protein-protein interactions in positive and negative control of pre-mRNA splicing by Transformer 2. *Cell* **76**, 735–746 (1994).
22. Wu, J. Y. & Maniatis, T. Specific interactions between proteins implicated in splice site selection and regulated alternative splicing. *Cell* **75**, 1061–1070 (1993).
23. Tian, M. & Maniatis, T. A splicing enhancer exhibits both constitutive and regulated activities. *Genes Dev.* **8**, 1703–1712 (1994).
24. Lynch, K. W. & Maniatis, T. Synergistic interactions between two distinct elements of a regulated splicing enhancer. *Genes Dev.* **9**, 284–293 (1995).
25. Lynch, K. W. & Maniatis, T. Assembly of specific SR protein complexes on distinct regulatory elements of the Drosophila doublesex splicing enhancer. *Genes Dev.* **10**, 2089–2101 (1996).
26. Heinrichs, V., Ryner, L. C. & Baker, B. S. Regulation of sex-specific selection of fruitless 5′ splice sites by transformer and transformer-2. *Mol. Cell Biol.* **18**, 450–458 (1998).
27. Sciabica, K. S. & Hertel, K. J. The splicing regulators Tra and Tra2 are unusually potent activators of pre-mRNA splicing. *Nucleic Acids Res* **34**, 6612–6620 (2006).
28. Zuo, P. & Maniatis, T. The splicing factor U2AF35 mediates critical protein-protein interactions in constitutive and enhancer-dependent splicing. *Genes Dev.* **10**, 1356–1368 (1996).
29. Dauwalder, B. & Mattox, W. Analysis of the functional specificity of RS domains in vivo. *EMBO J.* **17**, 6049–6060 (1998).
30. Baker, B. S. & Wolfner, M. F. A molecular analysis of doublesex, a bifunctional gene that controls both male and female sexual differentiation in Drosophila melanogaster. *Genes Dev.* **2**, 477–489 (1988).
31. Burtis, K. C. & Baker, B. S. Drosophila doublesex gene controls somatic sexual differentiation by producing alternatively spliced mRNAs encoding related sex-specific polypeptides. *Cell* **56**, 997–1010 (1989).
32. Ito, H. et al. Sexual orientation in Drosophila is altered by the satori mutation in the sex-determination gene fruitless that encodes a zinc finger protein with a BTB domain. *Proc. Natl Acad. Sci. USA* **93**, 9687–9692 (1996).
33. Ryner, L. C. et al. Control of male sexual behavior and sexual orientation in Drosophila by the fruitless gene. *Cell* **87**, 1079–1089 (1996).
34. Lee, G. et al. Spatial, temporal, and sexually dimorphic expression patterns of the fruitless gene in the Drosophila central nervous system. *J. Neurobiol.* **43**, 404–426 (2000).
35. Goodwin, S. F. et al. Aberrant splicing and altered spatial expression patterns in fruitless mutants of Drosophila melanogaster. *Genetics* **154**, 725–745 (2000).
36. Demir, E. & Dickson, B. J. fruitless splicing specifies male courtship behavior in Drosophila. *Cell* **121**, 785–794 (2005).
37. Manoli, D. S. et al. Male-specific fruitless specifies the neural substrates of Drosophila courtship behaviour. *Nature* **436**, 395–400 (2005).
38. Kimura, K.-I., Ote, M., Tazawa, T. & Yamamoto, D. Fruitless specifies sexually dimorphic neural circuitry in the Drosophila brain. *Nature* **438**, 229–233 (2005).
39. Shirangi, T. R., Taylor, B. J. & McKeown, M. A double-switch system regulates male courtship behavior in male and female Drosophila melanogaster. *Nat. Genet* **38**, 1435–1439 (2006).
40. Rideout, E. J., Billeter, J.-C. & Goodwin, S. F. The sex-determination genes fruitless and doublesex specify a neural substrate required for courtship song. *Curr. Biol.* **17**, 1473–1478 (2007).
41. Clough, E. et al. Sex- and tissue-specific functions of Drosophila doublesex transcription factor target genes. *Dev. Cell* **31**, 761–773 (2014).
42. Sato, K. & Yamamoto, D. Molecular and cellular origins of behavioral sex differences: a tiny little fly tells a lot. *Front Mol. Neurosci.* **16**, 1284367 (2023).
43. Nojima, T. et al. A sex-specific switch between visual and olfactory inputs underlies adaptive sex differences in behavior. *Curr. Biol.* **31**, 1175–1191.e6 (2021).
44. Rideout, E. J., Dornan, A. J., Neville, M. C., Eadie, S. & Goodwin, S. F. Control of sexual differentiation and behavior by the doublesex gene in Drosophila melanogaster. *Nat. Neurosci.* **13**, 458–466 (2010).
45. Burtis, K. C., Coschigano, K. T., Baker, B. S. & Wensink, P. C. The doublesex proteins of Drosophila melanogaster bind directly to a sex-specific yolk protein gene enhancer. *EMBO J.* **10**, 2577–2582 (1991).
46. Shirangi, T. R., Dufour, H. D., Williams, T. M. & Carroll, S. B. Rapid evolution of sex pheromone-producing enzyme expression in Drosophila. *PLoS Biol.* **7**, e1000168 (2009).
47. Camara, N., Whitworth, C., Dove, A. & Van Doren, M. Doublesex controls specification and maintenance of the gonad stem cell niches in Drosophila. *Development* **146**, dev170001 (2019).
48. Robinett, C. C., Vaughan, A. G., Knapp, J.-M. & Baker, B. S. Sex and the single cell. II. There is a time and place for sex. *PLoS Biol.* **8**, e1000365 (2010).
49. Pan, Y., Robinett, C. C. & Baker, B. S. Turning males on: activation of male courtship behavior in Drosophila melanogaster. *PLoS One* **6**, e21144 (2011).
50. Stockinger, P., Kvitsiani, D., Rotkopf, S., Tirián, L. & Dickson, B. J. Neural circuitry that governs Drosophila male courtship behavior. *Cell* **121**, 795–807 (2005).
51. Belote, J. M., Handler, A. M., Wolfner, M. F., Livak, K. J. & Baker, B. S. Sex-specific regulation of yolk protein gene expression in Drosophila. *Cell* **40**, 339–348 (1985).
52. Bownes, M., Scott, A. & Blair, M. The use of an inhibitor of protein synthesis to investigate the roles of ecdysteroids and sex-determination genes on the expression of the genes encoding the Drosophila yolk proteins. *Development* **101**, 931–941 (1987).
53. Grmai, L., Hudry, B., Miguel-Aliaga, I. & Bach, E. A. Chinmo prevents transformer alternative splicing to maintain male sex identity. *PLoS Genet* **14**, e1007203 (2018).

54. Peng, Q., Chen, J. & Pan, Y. From fruitless to sex: On the generation and diversification of an innate behavior. *Genes Brain Behav*. **20**, e12772 (2021).
55. Chen, J. et al. fruitless tunes functional flexibility of courtship circuitry during development. *Elife* **10**, e59224 (2021).
56. Peng, Q. et al. The sex determination gene doublesex is required during adulthood to maintain sexual orientation. *J. Genet Genomics* **49**, 165–168 (2022).
57. Bayer, E. A., Sun, H., Rafi, I. & Hobert, O. Temporal, spatial, sexual and environmental regulation of the master regulator of sexual differentiation in C. elegans. *Curr. Biol.* **30**, 3604–3616.e3 (2020).
58. Lawson, H. N., Wexler, L. R., Wnuk, H. K. & Portman, D. S. Dynamic, non-binary specification of sexual state in the c. elegans nervous system. *Curr. Biol.* **30**, 3617–3623.e3 (2020).
59. Rideout, E. J., Narsaiya, M. S. & Grewal, S. S. The sex determination gene transformer regulates male-female differences in drosophila body size. *PLoS Genet* **11**, e1005683 (2015).
60. Wat, L. W., Chowdhury, Z. S., Millington, J. W., Biswas, P. & Rideout, E. J. Sex determination gene transformer regulates the male-female difference in Drosophila fat storage via the adipokinetic hormone pathway. *Elife* **10**, e72350 (2021).
61. Regan, J. C. et al. Sex difference in pathology of the ageing gut mediates the greater response of female lifespan to dietary restriction. *Elife* **5**, e10956 (2016).
62. Hudry, B., Khadayate, S. & Miguel-Aliaga, I. The sexual identity of adult intestinal stem cells controls organ size and plasticity. *Nature* **530**, 344–348 (2016).
63. Hudry, B. et al. Sex differences in intestinal carbohydrate metabolism promote food intake and sperm maturation.*Cell* **178**, 901–918.e16 (2019).
64. Ma, J. & Ptashne, M. The carboxy-terminal 30 amino acids of GAL4 are recognized by GAL80. *Cell* **50**, 137–142 (1987).
65. Baena-Lopez, L. A., Alexandre, C., Mitchell, A., Pasakarnis, L. & Vincent, J.-P. Accelerated homologous recombination and subsequent genome modification in Drosophila. *Development* **140**, 4818–4825 (2013).
66. Cline, T. W. Autoregulatory functioning of a Drosophila gene product that establish es and maintains the sexually determined state. *Genetics* **107**, 231–277 (1984).
67. Testa, N. D., Ghosh, S. M. & Shingleton, A. W. Sex-specific weight loss mediates sexual size dimorphism in Drosophila melanogaster. *PLoS One* **8**, e58936 (2013).
68. Geuverink, E. & Beukeboom, L. W. Phylogenetic distribution and evolutionary dynamics of the sex determination genes doublesex and transformer in insects. *Sex. Dev.* **8**, 38–49 (2014).
69. Whitfield, L. S., Lovell-Badge, R. & Goodfellow, P. N. Rapid sequence evolution of the mammalian sex-determining gene SRY. *Nature* **364**, 713–715 (1993).
70. Pamilo, P. & O'Neill, R. J. Evolution of the Sry genes. *Mol. Biol. Evol.* **14**, 49–55 (1997).
71. O'Neil, M. T. & Belote, J. M. Interspecific comparison of the transformer gene of Drosophila reveals an unusually high degree of evolutionary divergence. *Genetics* **131**, 113–128 (1992).
72. Shukla, J. N. & Palli, S. R. Sex determination in beetles: production of all male progeny by parental RNAi knockdown of transformer. *Sci. Rep.* **2**, 602 (2012).
73. Meissner, G. W., Luo, S. D., Dias, B. G., Texada, M. J. & Baker, B. S. Sex-specific regulation of Lgr3 in Drosophila neurons. *Proc. Natl Acad. Sci. USA* **113**, E1256–E1265 (2016).
74. Bussell, J. J., Yapici, N., Zhang, S. X., Dickson, B. J. & Vosshall, L. B. Abdominal-B neurons control Drosophila virgin female receptivity. *Curr. Biol.* **24**, 1584–1595 (2014).
75. Estrada, B. & Sánchez-Herrero, E. The Hox gene Abdominal-B antagonizes appendage development in the genital disc of Drosophila. *Development* **128**, 331–339 (2001).
76. Foronda, D., Estrada, B., de Navas, L. & Sánchez-Herrero, E. Requirement of Abdominal-A and Abdominal-B in the developing genitalia of Drosophila breaks the posterior downregulation rule. *Development* **133**, 117–127 (2006).
77. Diao, F. et al. Plug-and-play genetic access to drosophila cell types using exchangeable exon cassettes. *Cell Rep.* **10**, 1410–1421 (2015).
78. Zhang, Z., Bae, B., Cuddleston, W. H. & Miura, P. Coordination of alternative splicing and alternative polyadenylation revealed by targeted long read sequencing. *Nat. Commun.* **14**, 5506 (2023).
79. Alfonso-Gonzalez, C. et al. Sites of transcription initiation drive mRNA isoform selection. *Cell* **186**, 2438–2455.e22 (2023).
80. Zheng, X. et al. Incompatible and sterile insect techniques combined eliminate mosquitoes. *Nature* **572**, 56–61 (2019).
81. Millington, J. W. et al. Female-biased upregulation of insulin pathway activity mediates the sex difference in Drosophila body size plasticity. *Elife* **10**, e58341 (2021).
82. Sawala, A. & Gould, A. P. The sex of specific neurons controls female body growth in Drosophila. *PLoS Biol.* **15**, e2002252 (2017).
83. Sawala, A. & Gould, A. P. Sex-lethal in neurons controls female body growth in Drosophila. *Fly. (Austin)* **12**, 133–141 (2018).
84. Belmonte, R. L., Corbally, M.-K., Duneau, D. F. & Regan, J. C. Sexual Dimorphisms in Innate Immunity and Responses to Infection in Drosophila melanogaster. *Front Immunol.* **10**, 3075 (2019).
85. Mank, J. E. & Rideout, E. J. Developmental mechanisms of sex differences: from cells to organisms. *Development* **148**, dev199750 (2021).
86. Goodfellow, P. N. & Lovell-Badge, R. SRY and sex determination in mammals. *Annu Rev. Genet* **27**, 71–92 (1993).
87. Lee, J. & Harley, V. R. The male fight-flight response: a result of SRY regulation of catecholamines? *Bioessays* **34**, 454–457 (2012).
88. Bellott, D. W. et al. Mammalian Y chromosomes retain widely expressed dosage-sensitive regulators. *Nature* **508**, 494–499 (2014).
89. Trabzuni, D. et al. Widespread sex differences in gene expression and splicing in the adult human brain. *Nat. Commun.* **4**, 2771 (2013).
90. Xu, J., Burgoyne, P. S. & Arnold, A. P. Sex differences in sex chromosome gene expression in mouse brain. *Hum. Mol. Genet* **11**, 1409–1419 (2002).
91. Johansson, M. M. et al. Spatial sexual dimorphism of X and Y homolog gene expression in the human central nervous system during early male development. *Biol. Sex. Differ.* **7**, 5 (2016).
92. Godfrey, A. K. et al. Quantitative analysis of Y-Chromosome gene expression across 36 human tissues. *Genome Res* **30**, 860–873 (2020).
93. Qi, M., Pang, J., Mitsiades, I., Lane, A. A. & Rheinbay, E. Loss of chromosome Y in primary tumors. *Cell* S0092-8674(23)00646–3 https://doi.org/10.1016/j.cell.2023.06.006 (2023).
94. Li, J. et al. Histone demethylase KDM5D upregulation drives sex differences in colon cancer. *Nature* **619**, 632–639 (2023).
95. Abdel-Hafiz, H. A. et al. Y chromosome loss in cancer drives growth by evasion of adaptive immunity. *Nature* **619**, 624–631 (2023).
96. Trotta, V., Calboli, F. C. F., Ziosi, M. & Cavicchi, S. Fitness variation in response to artificial selection for reduced cell area, cell number and wing area in natural populations of Drosophila melanogaster. *BMC Evol. Biol.* **7**, S10 (2007).

Acknowledgements

We thank Carolina Rezaval, and Benjamin Prud'homme for fly lines; the Bloomington *Drosophila* Stock Centre for providing *Drosophila* fly lines; the iBV platforms: Baptiste Monterroso and Sameh Ben Aicha from the imaging facility, Florence Besse and Romain Levayer for comments and Anita Mencser for fly food; and all the members of the BH laboratory for fruitful discussions and comments. We would like to express our gratitude to Irene Miguel-Aliaga for her support at the start of the project. This work was supported by the Université Côte d'Azur, CNRS (ATIP-Avenir programme), INSERM, European Research Council (ERC starting grant CellSex, Grant number: ERC-2019-STG#850934), and the French

Government (National Research Agency, ANR) through the "Investments for the Future" programmes LABEX SIGNALIFE ANR-11-LABX-0028-01 and IDEX UCAJedi ANR-15-IDEX-01.

Author contributions

Conceptualisation: C.H. and B.H. Methodology: C.H. and B.H. Investigation: C.H. and T.P. Visualisation: C.H. Funding acquisition: B.H. Project administration: B.H. Supervision: B.H. Writing – original draft: B.H.

Competing interests

The authors declare no competing interests.

Additional information

Supplementary information The online version contains supplementary material available at https://doi.org/10.1038/s41467-024-51228-6.

Correspondence and requests for materials should be addressed to Bruno Hudry.

Peer review information *Nature Communications* thanks the anonymous reviewers for their contribution to the peer review of this work. A peer review file is available.